Acta Cryst. (1999). B**55**, 85–94

Structures of 2,6-disubstituted naphthalenes

James A. Kaduk* and Joseph T. Golab

Amoco Corporation, PO Box 3011, MC F-9 Naperville, IL 60566, USA. E-mail: kaduk@amoco.com

(*Received 9 October 1997; accepted 29 June 1998*)

Abstract

The crystal structures of 2,6-naphthalenedicarboxylic acid (NDA) and dimethyl 2,6-naphthalenedicarboxylate (NDC) have been solved *ab initio* using a combination of X-ray powder diffraction and computational chemistry techniques. These two crystal structures, and that of 2,6-dimethylnaphthalene (DMN), have been refined by the Rietveld technique. DMN crystallizes in the orthorhombic space group *Pbca*, with a = 7.4544 (4), b = 6.0826 (6), c = 20.0946 (12) Å, V = 911.1 (1) Å^3 and Z = 4. The structure consists of a herringbone stacking parallel to **a**, resulting in loosely bound layers perpendicular to **c**. NDA crystallizes in the triclinic space group $P\bar{1}$, with a = 3.7061 (8), b = 7.4688 (14), c = 8.5352 (22) Å, α = 86.62 (2), β = 85.49 (2), γ = 87.99 (2)°, V = 235.00 (6) Å^3 and Z = 1. The structure consists of loosely packed hydrogen-bonded chains along [1$\bar{1}$1]. NDC crystallizes in the monoclinic space group $P2_1/c$, with a = 13.41931 (14), b = 6.14869 (5), c = 7.15257 (5) Å, β = 100.400 (1)°, V = 580.47 (1) Å^3 at 300 K and Z = 2. The structure consists of layers of NDC molecules perpendicular to **a**. The ester group is twisted 20° out of the mean ring plane in NDC. The conformations of the carboxyl groups in NDA and NDC differ. MP2 calculations suggest that the observed twist in NDC corresponds to an increase in conformational energy of 9 kJ mol^{-1}.

1. Introduction

Poly(ethylene 2,6-naphthalenedicarboxylate), PEN, is a promising polymer for use in applications requiring superior physical properties to those of poly(ethylene terephthalate), PET (Morse, 1997). The commercial monomer, dimethyl 2,6-naphthalenedicarboxylate (NDC), is prepared by esterification of 2,6-naphthalenedicarboxylic acid (NDA), which is obtained by homogeneous oxidation of 2,6-dimethylnaphthalene (DMN).

Although an approximate crystal structure of 2,6-dimethylnaphthalene has been reported by Kitaigorodskii (1946, 1953; refcode DMNPTL), the crystal structures of NDA and NDC have not yet been determined. Recent advances in powder diffraction and computational chemistry techniques have made it possible to solve structures *ab initio* using powder diffraction data. Knowledge of the crystal structures permits quantitative phase analysis and characterization of microstructural properties (texture, defects, strain, domain size *etc.*) using Rietveld refinement techniques.

This paper reports a new refinement of the crystal structure of DMN, as well as the *ab initio* solution and refinement of the structures of NDA and NDC using a combination of powder diffraction and computational chemistry techniques.

2. Experimental

2.1. *2,6-Dimethylnaphthalene (DMN)*

A sample of commercial DMN was mixed with 5.88 wt% NIST 640b Si internal standard and ground in a McCrone micronizing mill using corundum grinding media and ethanol as the milling liquid; we have as yet been unable to grow suitable single crystals. The white powder was packed into a 50 μm-deep zero-background quartz sample cell and the X-ray powder diffraction pattern was measured at 293 K on a Scintag PAD V diffractometer (Cu $K\alpha$ radiation; $\lambda_{\alpha1}$ = 1.540629, $\lambda_{\alpha2}$ = 1.544451 Å) from 2θ = 3 to 80° in 0.02° steps, counting for 12 s per step. The observed pattern corresponded to the Powder Diffraction File entry 17-1014 for DMN.

The reported structure of DMN (Kitaigorodskii, 1946, 1953; refcode DMNPTL) is distorted, but was suitable as a starting point for a Rietveld refinement. The pattern calculated from the entry DMNPTL in the Cambridge Structural Database (CSD; Allen & Kennard, 1993), however, did not correspond to the observed pattern. Only some of the peaks appeared in the observed positions. The pattern of a thin smear of material on a zero-background cell yielded peak positions sufficiently precise for the pattern to be indexed (Boultif & Louer, 1991) on a primitive orthorhombic cell having a = 7.454 (3), b = 6.073 (3) and c = 20.098 (13) Å. The cell dimensions in the CSD entry DMNPTL are a = 4.54, b = 6.07 and c = 20.20 Å, while the lattice parameters in the *Structure Reports* entry for this structure are a = 7.54, b = 6.07 and c = 20.20 Å. When the correct cell parameters were used in the calculation of the pattern, much better agreement with the observed pattern was obtained.

All data processing was carried out using *GSAS* (Larson & Von Dreele, 1994). To minimize the effects of surface roughness and incomplete interception of the

beam at low angles, only the $2\theta = 20$–80° portion of the pattern was included in the refinement. The reported structure was used as the basis for the refinement. The five unique atoms of the naphthalene core (the molecule resides on a center of symmetry in space group *Pbca*) were described as a rigid body, with a C—C bond distance of 1.392 Å. A soft constraint of 1.39 (1) Å was applied to the C1—C5^{i} and C5—C5^{i} bonded distances, and a constraint of 2.43 (1) Å was applied to the nonbonded C2···C5^{i}, C4···C5^{i} and C4···C1^{i} distances in the center of the molecule. A soft constraint of 1.50 (1) Å was applied to the C2—C6 distance and constraints of 2.53 (1) Å to the C6···C1 and C6···C3 distances. H atoms were included in calculated positions, which were updated during the course of the refinement. A common isotropic displacement coefficient was refined for the C atoms.

Both the silicon internal standard and a corundum impurity (a contaminant from the grinding medium of the micronizing mill) were included using fixed structural models. Scale factors for each phase, as well as the lattice parameters for DMN and corundum, were refined. The DMN pattern exhibited a pronounced (001) preferred orientation, which was described using a March–Dollase model. The profiles were described using a pseudo-Voigt function. For DMN, only the Gaussian *U*, Cauchy *Y* and *stec* (unique axis 001) strain broadening terms were refined. A common sample displacement term was included. The background was described by a three-term cosine Fourier series.

The final refinement of 28 variables using 3008 observations yielded the residuals $R_{wp} = 0.1086$, $R_p = 0.0852$, $\chi^2 = 11.84$ and $R(F) = 0.0689$. The agreement of the observed and calculated patterns (Fig. 1) is good. The largest errors are in the description of the asymmetry of the low-angle peaks. The largest peak in the final difference Fourier map was 0.17 e Å^{-3} and the largest difference hole was −0.21 e Å^{-3}. A normal probability plot indicated that the standard uncertainties are underestimated by a factor of 2.9. The refined structural parameters are reported in Table 1. The bond distances and angles are listed in Table 2.

Table 1. *Fractional atomic coordinates and isotropic displacement parameters (Å^2) for DMN*

	x	*y*	*z*	U_{iso}
C1	0.0747 (7)	−0.2245 (5)	0.05524 (16)	0.0327 (14)
C2	0.0291	−0.1401	0.11735	0.0327
C3	−0.0501	0.0665	0.12223	0.0327
C4	−0.0836	0.1887	0.06499	0.0327
C5	−0.0379	0.1043	0.00288	0.0327
C6	0.0691 (9)	−0.2765 (11)	0.1796 (2)	0.0327
H1	0.13727	−0.36194	0.05223	0.05
H3	−0.08499	0.12338	0.16486	0.05
H4	−0.14077	0.32956	0.06804	0.05
H6*a*	0.02582	−0.19759	0.21882	0.05
H6*b*	0.00317	−0.41330	0.17655	0.05
H6*c*	0.19233	−0.30354	0.18314	0.05

Table 2. *Selected geometric parameters (Å, °) for DMN*

C2—C1	1.392†	C2—C3	1.392†
C2—C6	1.530 (3)‡	C3—C4	1.392†
C4—C5	1.392†	C5—C5^{i}	1.394 (4)‡
C5—C1^{i}	1.405 (3)‡		
C3—C2—C1	120†	C3—C2—C6	121.0 (3)‡
C1—C2—C6	119.0 (3)‡	C2—C3—C4	120†
C3—C4—C5	120†	C4—C5—C5^{i}	120.6 (1)‡
C4—C5—C1^{i}	120.4 (2)‡	C5—C5^{i}—C1	119.0 (2)‡
C2—C1—C5^{i}	120.4 (2)‡		

Symmetry code: (i) $-x, -y, -z$. † Constrained as part of the rigid body. ‡ Restrained by soft constraints.

2.2. *2,6-Naphthalenedicarboxylic acid (NDA)*

NDA is exceptionally difficult to crystallize. Of all the 'single crystals' we have examined, only one has been

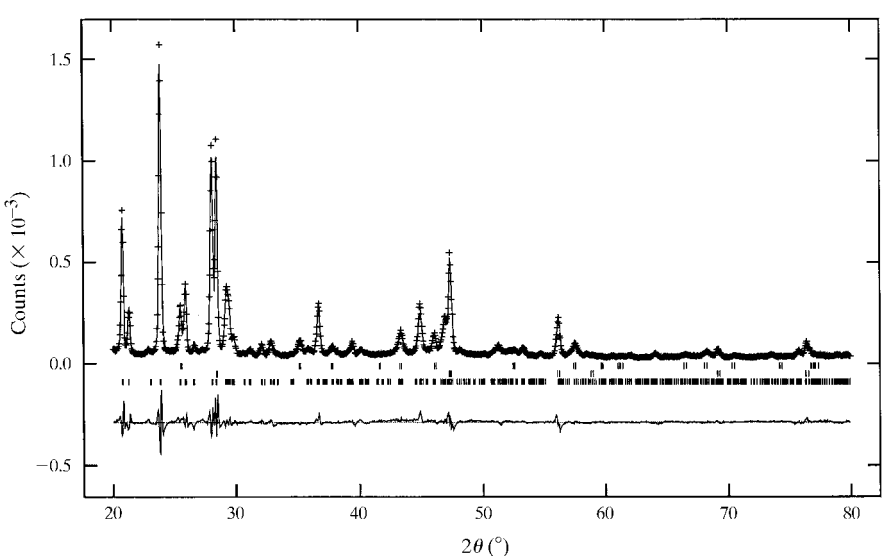

Fig. 1. Observed, calculated, and difference patterns of DMN. The small crosses represent the observed data points and the solid line through them the calculated pattern. The difference curve is plotted on the same scale as the other patterns. The bottom row of tick marks represents the positions of the DMN peaks, the middle row indicates the positions of the Si internal standard peaks and the top row indicates the positions of the corundum impurity peaks.

indexable as a single crystal: on a triclinic unit cell having $a = 3.7100$ (8), $b = 7.4337$ (42), $c = 8.6111$ (47) Å, $\alpha = 86.291$ (44), $\beta = 85.640$ (33), $\gamma = 88.745$ (35)° and $V = 236.3$ (2) Å^3. A single-crystal dataset was collected, but the structure proved to be badly disordered.

An exceptionally crystalline sample of NDA was obtained from the commercial plant. The powder pattern showed peak positions consistent with the above triclinic unit cell. The white powder was mounted in a zero-background cell and the pattern measured at 293 K on a Scintag PAD V diffractometer (Cu $K\alpha$ radiation, $\lambda_{\alpha1} = 1.540629$, $\lambda_{\alpha2} = 1.544451$ Å) from $2\theta = 3$ to 60° in 0.02° steps, counting for 10 s per step.

The density is such that there must be one molecule per unit cell. On the reasonable assumption that the molecule is centrosymmetric, the space group is $P\bar{1}$, and the molecule occupies a center of symmetry. The location of the molecule in the unit cell was therefore known and 'only' the orientation needed to be determined.

The short a unit-cell dimension places severe limits on the possible orientation of the molecule in the cell. Since it was virtually certain that the molecules would form hydrogen-bonded chains, the *Cerius*[2] package (Molecular Simulations Inc., 1995) was used to orient the molecule to form such chains. The size and shape of the unit cell were consistent only with such chains in the $[1\bar{1}1]$ direction. This approximate model, derived only from packing considerations, was used to generate a rigid half molecule as an initial model for a Rietveld refinement.

All data processing was carried out using *GSAS* (Larson & Von Dreele, 1994). The five unique C atoms of the naphthalene core were refined as a rigid body. Soft constraints of 1.39 (1) and 2.43 (1) Å were applied to the bonded and nonbonded distances in the center of the naphthalene core. Constraints of 1.51 (1), 1.28 (1) and 1.28 (1) Å were applied to the C2—C7, C7—O1 and C7—O2 bonds. The refined distances made it very clear that C7—O2 was the C—O single bond and that C7—O1 was the C═O double bond. The soft constraints (including nonbonded distances) were then adjusted to correspond to the NDA geometry of this conformation calculated using *SYBYL* (Tripos Associates Inc., 1994). H atoms were included in calculated positions, which were updated during the course of the refinement. Attempts to refine the isotropic displacement coefficients of the non-H atoms led to large values (larger for the core atoms than for the carboxyls) and U_{iso}'s were fixed at 0.05 Å^2.

A scale factor and the lattice parameters were refined. A March–Dollase preferred orientation ratio (unique axis 011) was refined. The profiles were described using a pseudo-Voigt function; only the Cauchy X and *ptec* (unique axis 011) size-broadening terms refined to values different than those of the instrumental profile function. The background was described using a three-term cosine Fourier series.

Table 3. *Fractional atomic coordinates and isotropic displacement parameters (Å^2) for NDA*

	x	y	z	U_{iso}
C1	0.6185 (48)	0.2666 (5)	0.5718 (10)	0.05
C2	0.6628	0.2945	0.7289	0.05
C3	0.6355	0.4675	0.7819	0.05
C4	0.5639	0.6126	0.6779	0.05
C5	0.5196	0.5848	0.5208	0.05
C7	0.7631 (50)	0.1425 (12)	0.8485 (11)	0.05
O1	0.915 (4)	0.0095 (13)	0.8015 (12)	0.05
O2	0.889 (4)	0.2036 (11)	0.9812 (11)	0.05
H1	0.69502	0.15599	0.52971	0.08
H2	0.9539	0.1334	1.0558	0.08
H3	0.67204	0.49483	0.88873	0.08
H4	0.54191	0.73661	0.71097	0.08

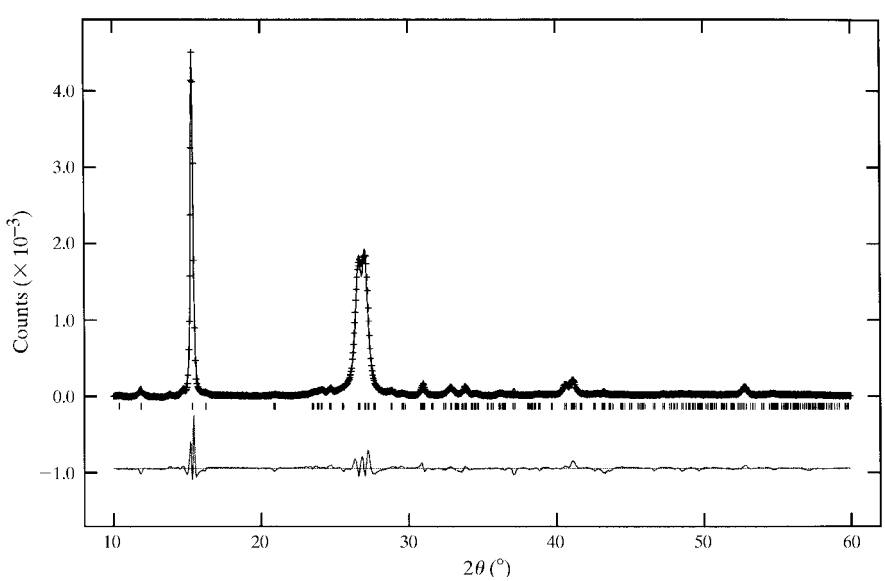

Fig. 2. Observed, calculated and difference patterns of NDA. The small crosses represent the observed data points and the solid line through them the calculated pattern. The difference curve is plotted at the same scale as the other patterns. The row of tick marks represents the positions of the NDA peaks.

Table 4. *Selected geometric parameters (Å, °) for NDA*

C2—C1	1.392†	C2—C3	1.392†
C2—C7	1.537 (6)‡	C1—C5^{i}	1.428 (7)‡
C3—C4	1.392†	C4—C5	1.392†
C5—C5^{i}	1.351 (8)‡	C7—O1	1.198 (9)‡
C7—O2	1.366 (9)‡		
C2—C1—C5^{i}	116.8 (5)‡	C1—C2—C3	120†
C1—C2—C7	123.0 (5)‡	C3—C2—C7	116.9 (6)‡
C2—C3—C4	120†	C3—C4—C5	120†
C4—C5—C5^{i}	118.4 (5)‡	C4—C5—C1^{i}	120.3 (5)‡
C2—C7—O1	119.0 (9)‡	C2—C7—O2	113.0 (9)‡
O1—C7—O2	115.1 (9)‡		

Symmetry code: (i) $1-x, 1-y, 1-z$. † Constrained as part of the rigid body. ‡ Restrained by soft constraints.

The final refinement of 28 variables using 2513 observations yielded the residuals $R_{wp} = 0.1422$, $R_p = 0.1056$, $\chi^2 = 36.00$ and $R(F) = 0.1027$. Agreement between the observed and calculated patterns (Fig. 2) is good. The largest errors are in the description of the asymmetry of the low-angle peaks. The largest peak in the final difference Fourier map was 0.33 e Å^{-3} (near C5) and the largest difference hole was −0.29 e Å^{-3}. A normal probability plot indicated that the standard uncertainties are underestimated by a factor of 4.9. The refined structural parameters are reported in Table 3 and the bond distances and angles are listed in Table 4.

2.3. *Dimethyl 2,6-naphthalenedicarboxylate (NDC)*

A sample of commercial material was ground in a McCrone micronizing mill, using corundum grinding media and ethanol as the milling liquid. For business reasons, it was important to characterize commercial material; we have not yet succeeded in growing suitable single crystals. The powder was packed into a sample cell and coated with clear automotive lacquer. The X-ray powder diffraction pattern was measured on a Scintag PAD V diffractometer from $2\theta = 3$ to 70° in 0.02° steps, counting for 4 s per step. The sample was rotated about the diffraction vector during the measurement.

The pattern could be indexed (Visser, 1969) on a high-quality primitive monoclinic unit cell having $a = 13.404$, $b = 6.169$, $c = 7.170$ Å and $\beta = 100.36°$. The systematic absences unambiguously determined the space group to be $P2_1/c$. The density is such that $Z = 2$ and thus that the molecule resides on a center of symmetry. The b and c lattice parameters are very similar to two of the cell dimensions of 2,6-dimethylnaphthalene, providing evidence that the stacking of the naphthalene cores is similar in the two structures. The lattice parameter a indicates that the long axis of the molecule is aligned roughly in this direction. A set of structure factors ($d > 1.60$ Å) obtained from a LeBail extraction was used as input to a direct methods (Sheldrick, 1988) calculation. This calculation indicated a preference for the orientation of the planar molecule with respect to rotation about the b axis, but no other clear indication of the crystal structure.

All this information was used to guide manipulation of the molecule in *Cerius*^{2} (Molecular Simulations Inc., 1995), monitoring the calculated diffraction pattern and assessing its similarity to the observed pattern, as well as monitoring intermolecular contacts. The problem was made more complex by the fact that there are two potential centrosymmetric conformations of the molecule. The *E* conformer was tried first. While plausible structures could be found, none of them could be refined successfully and the molecules did not really pack together very well. Changing to the *Z* conformer quickly

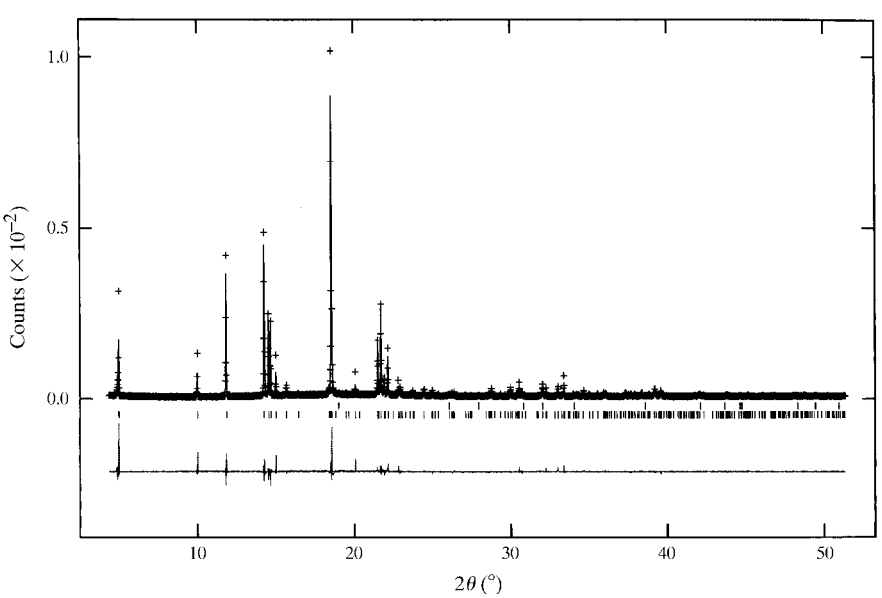

Fig. 3. Observed, calculated and difference patterns of NDC. The small crosses represent the observed data points and the solid line through them the calculated pattern. The difference curve is plotted on the same scale as the other patterns. The bottom row of tick marks represents the positions of the NDC peaks and the top row indicates the positions of the corundum impurity peaks.

Table 5. *Fractional atomic coordinates and isotropic displacement parameters (Å²) for NDC*

	x	*y*	*z*	U_{iso}
C1	−0.1040 (2)	−0.1874 (4)	−0.1007 (5)	0.018 (1)
C2	−0.1894	−0.0634	−0.0889	0.018
C3	−0.1786	0.1450	−0.0118	0.018
C4	−0.0824	0.2294	0.0536	0.018
C5	0.0030	0.1054	0.0418	0.018
C7	−0.2961 (4)	−0.1447 (9)	−0.1564 (9)	0.065 (1)
C8	−0.3995 (5)	−0.4521 (8)	−0.2158 (9)	0.065
O1	−0.3679 (4)	−0.0283 (5)	−0.1824 (6)	0.065
O2	−0.2968 (4)	−0.3610 (6)	−0.1662 (6)	0.065
H1	−0.10988	−0.32732	−0.16292	0.08
H3	−0.23656	0.22009	0.00727	0.08
H4	−0.07469	0.36332	0.11918	0.08
H8*a*	−0.39678	−0.60428	−0.22005	0.08
H8*b*	−0.43334	−0.40741	−0.11185	0.08
H8*c*	−0.43400	−0.39121	−0.33000	0.08

Table 6. *Selected geometric parameters (Å, °) for NDC*

C2—C1	1.392†	C2—C3	1.392†
C2—C7	1.510 (5)‡	C3—C4	1.392†
C4—C5	1.392†	C5—C5^{i}	1.423 (5)‡
C5—C1^{i}	1.436 (4)‡	C7—O1	1.188 (5)‡
C7—O2	1.332 (5)‡	O2—C8	1.470 (5)‡
C1—C2—C3	120†	C1—C2—C7	122.9 (2)‡
C3—C2—C7	117.1 (2)‡	C2—C3—C4	120†
C3—C4—C5	120†	C4—C5—C5^{i}	122.6 (1)‡
C4—C5—C1^{i}	122.3 (3)‡	C1^{i}—C5—C5^{i}	114.9 (3)‡
C2—C1—C5^{i}	122.3 (2)‡	C2—C7—O1	123.1 (5)‡
C2—C7—O2	110.2 (5)‡	O1—C7—O2	126.5 (5)‡
C7—O2—C8	113.0 (5)‡		

Symmetry code: (i) $-x, -y, -z$. † Constrained as part of the rigid body. ‡ Restrained by soft constraints.

resulted in identification of a promising low-energy structure, one which refined well in a Rietveld refinement.

Although the structure was solved using laboratory powder data, the final refinement was carried out using a pattern collected at beamline X3B1 at the National Synchrotron Light Source at Brookhaven National Laboratory. Another micronized sample of the white powder was packed tightly into a 1 mm glass capillary. The powder pattern was measured from 2θ = 4.000 to 51.370° in 0.003° steps, using a calibrated (NIST SRM 1976 alumina plate) wavelength of 1.15023 Å. The pattern was collected in two sections; for the 4.000–22.237° portion a counting time of 2 s per step was used, while 4 s per step was used for the high-angle portion of the pattern. At each data point the sample was rocked from $\omega - 4$ to $\omega + 4$°. The two patterns were normalized using the monitor counts and merged into a single *GSAS* format data file. Only the 4.370–51.370° portion of the pattern was included in the refinement.

Initial refinements with laboratory data used an eight-atom rigid body consisting of half the naphthalene core and the carboxyl group. After this converged a difference Fourier map was calculated. The two strongest peaks were located near the bridgehead C atoms, but the third strongest peak was in a reasonable location for the methyl carbon C8, in agreement with the orientation derived using *Cerius*[2] (Molecular Simulations Inc., 1995). The final refinements treated the five-atom half naphthalene core as a rigid body and used extensive soft constraints in the center and the ester linkage. H atoms were included in calculated positions, which were updated during the course of the refinement. A common isotropic displacement coefficient was refined for the core C atoms and a separate displacement parameter was refined for the ester group. The isotropic displacement coefficient of the H atoms was fixed at 0.08 Å².

This sample also contained a corundum impurity, a contaminant from the grinding media. Corundum was included in the refinement using a fixed structural model. Scale factors and the lattice parameters for both phases were refined. The NDC peaks exhibited preferred orientation, consistent with the layered structure. Second-order symmetrized spherical harmonic preferred orientation coefficients were refined. The profiles were described by pseudo-Voigt functions. The profiles were dominated by strain broadening. For NDC the Gaussian *U* and Cauchy *Y*, and L_{xy} anisotropic strain broadening parameters were refined; only the *Y* profile parameter was refined for corundum. The background from the capillary was described by a ten-term real-space pair correlation function, with fixed characteristic distances of 0.716, 3.883, 4.000 and 4.771 Å.

The final refinement of 49 variables using 15 683 observations yielded the residuals R_{wp} = 0.1152, R_p = 0.0912, χ^2 = 9.011 and $R(F)$ = 0.1855. Agreement between the observed and calculated patterns (Fig. 3) is good. The largest errors are in the description of the asymmetry of the low-angle peaks. The largest peak in the final difference Fourier map was 0.61 e Å^{-3} and the largest difference hole was −0.67 e Å^{-3}. A normal probability plot indicated that the standard uncertainties are underestimated by a factor of 2.3. The refined structural parameters are reported in Table 5, and the bond distances and angles are listed in Table 6. The powder patterns of all three compounds, calculated from the final coordinates, have been submitted to the International Centre for Diffraction Data for inclusion in the Powder Diffraction File (the PDF No. for NDA is 48-2483 and the PDF No. for NDC is 48-2484).†

3. Results

3.1. *Descriptions of the structures*

The crystal structure of 2,6-dimethylnaphthalene reported by Kitaigorodskii (1946, 1953; refcode

† Supplementary data for this paper are available from the IUCr electronic archives (Reference: BK0054). Services for accessing these data are described at the back of the journal.

DMNPTL) has been confirmed, to higher accuracy and precision. Since the molecule (Fig. 4) was refined as a rigid body and with soft constraints, all distances and angles fall within the expected ranges. The molecule is planar; all C atoms are within 0.02 Å of the mean plane.

The crystal structure consists of a herringbone stacking of the aromatic rings along the *a* axis (Fig. 5). This face-to-face stacking, along with side-to-side interactions, results in a layered structure, with the layers perpendicular to the *c* axis. There are no close methyl–methyl interactions; the shortest H···H distance is 2.38 Å (H6*a*—H3). The layers are very loosely bound, consistent with the plate-like morphology indicated by the March–Dollase preferred orientation ratio and the observed particle shapes. This is a typical packing of an aromatic hydrocarbon.

The crystal structure of 2,6-naphthalenedicarboxylic acid consists of centrosymmetric molecules (Fig. 6), linked by strong hydrogen bonds (O1···O2 = 2.51 Å) to form chains along [1$\bar{1}$1]. Since a rigid body and soft constraints were used, all the distances fall within the expected ranges. The molecule is apparently ruffled. The largest deviations from the mean core plane are 0.11 (C5) and 0.07 Å (C1). C7 is in the mean plane of the naphthalene core, but O1 and O2 are 0.48 and 0.26 Å out of plane. The angle between the mean core plane and the carboxyl plane is 36°, and the torsion angles C1—C2—C7—O1 and C3—C2—C7—O2 are 24 and −14°, respectively. The sums of the bond angles around C2 and C7 are 360 and 347°, respectively.

The crystal structure is best viewed approximately down the short *a* axis (Fig. 7). With the exception of the hydrogen bonds, the packing is dominated by van der Waals interactions. There are no close intermolecular contacts; the shortest H···H distance is 2.21 Å (H3—H3). The 'loose' packing (ρ_{calc} = 1.53 g cm^{-3}) can permit disorder. If the two carboxyl ends of the molecule are superimposed as closely as possible, two possible orientations for the naphthalene core can be accommodated. Such disorder is probably one factor contributing to the apparent distortions in the molecular geometry and to the very poor quality of 'single' crystals.

The crystal structure of dimethyl 2,6-naphthalenedicarboxylate contains discrete centrosymmetric molecules having the *Z* conformation (Fig. 8). Since a rigid body and soft constraints were used, all distances and angles fall within the expected ranges. The naphthalene core and the ester linkage are planar; the ring C atoms C1–C5 are within 0.0003 Å of the mean plane and the atoms of the ester group (C7, C8, O1 and O2) are within

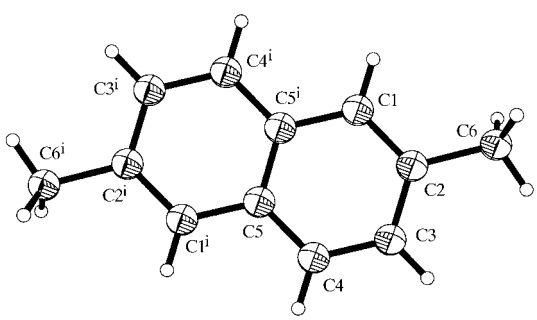

Fig. 4. The molecular structure of DMN, illustrating the atom-numbering scheme. The heavy atoms are represented by 50% probability spheroids and the H atoms by small circles of arbitrary radii. Symmetry code: (i) $-x, -y, -z$.

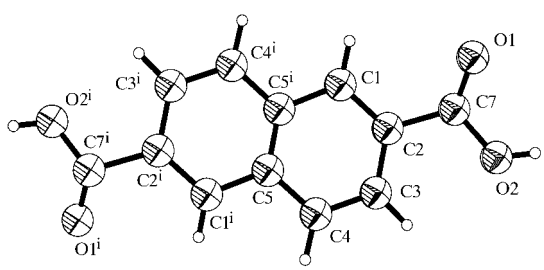

Fig. 6. The molecular structure of NDA, illustrating the atom-numbering scheme. The heavy atoms are represented by 50% probability spheroids and the H atoms by small circles of arbitrary radii. Symmetry code: (i) $1-x, 1-y, 1-z$.

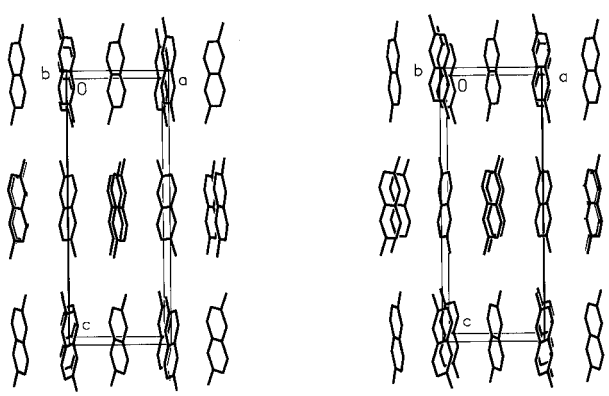

Fig. 5. The crystal structure of DMN, viewed down the *b* axis. H atoms have been omitted for clarity.

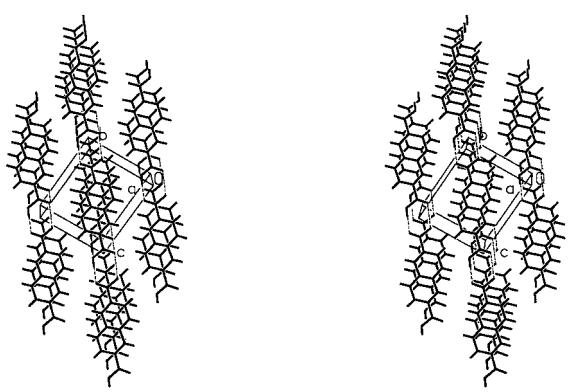

Fig. 7. The crystal structure of NDA, viewed approximately down the *a* axis (the aromatic ring planes are perpendicular to the view direction).

0.02 Å of the mean plane. The ester group is twisted out of the core plane; the C3—C2—C7═O1 torsion angle is 16°, the C1—C2—C7—O2 torsion angle is 20° and the angle between the mean planes is 20°.

The crystal structure (Fig. 9) consists of layers perpendicular to the *a* axis. The aromatic rings are inclined and stack parallel to **c**, with 'side-to-side' interactions along **b**. The molecules pack in a herringbone fashion in these directions, resulting in an interlocking layer. These layers interact only loosely with their neighbors along **a**, with only end-to-end contacts between the layers. This packing accounts for the plate-like morphology and the pronounced preferred orientation in flat-plate samples, even after extensive grinding. There are no close intermolecular contacts; the packing is dominated by van der Waals interactions.

3.2. *Statistical and theoretical studies*

A search of the CSD (Allen & Kennard, 1993) for aromatic carboxylic acids containing no *ortho* substituents yielded 261 hits. The average values of the geometric quantities of interest are summarized in Table 7. The observed quantities for NDA are similar, at least in part because of the soft constraints. The observed powder pattern strongly suggests the conformation reported here rather than that obtained by rotating the carboxyl groups by 180°; the soft constraints contribute only 10% of the final χ^2. Owing to ambiguities in the definitions of the torsion angle, it is best to consider the deviation of the torsion angle from 0/180° (the twist out

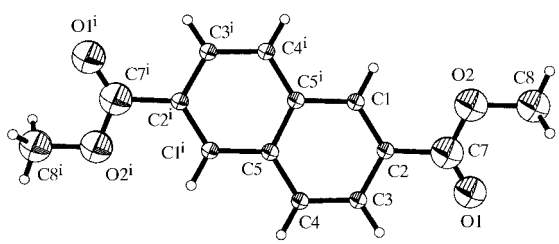

Fig. 8. The molecular structure of NDC, illustrating the atom-numbering scheme. The heavy atoms are represented by 50% probability spheroids and the H atoms by small circles of arbitrary radii. Symmetry code: (i) $-x, -y, -z$.

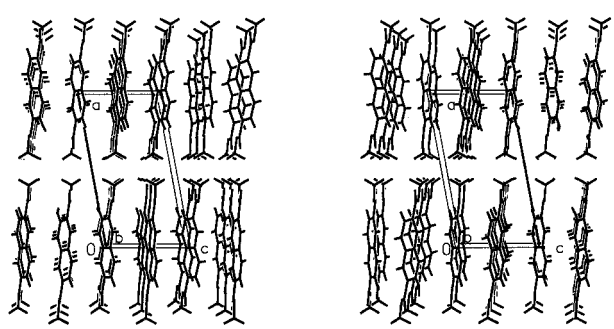

Fig. 9. The NDC crystal structure, viewed down the *b* axis.

Table 7. *Average (CSD) and experimental structural parameters for aromatic carboxylic acids*

Parameter	CSD average	NDA experimental
C2—C7 (Å)	1.483 (18)	1.537 (6)
C7═O1 (Å)	1.233 (26)	1.198 (9)
C7—O2 (Å)	1.294 (23)	1.366 (9)
C2—C7═O1 (°)	121.1 (21)	119.0 (9)
C2—C7—O2 (°)	115.6 (21)	113.0 (9)
O1—C7—O2 (°)	123.2 (13)	115.1 (9)
|C1—C2—C7═O1| (°)	5.3 (47)	24

Table 8. *Average (CSD) and experimental structural parameters for aromatic methyl esters*

Parameter	CSD average	NDC experimental
C2—C7 (Å)	1.487 (12)	1.510 (5)
C7═O1 (Å)	1.199 (12)	1.188 (5)
C7—O2 (Å)	1.331 (12)	1.332 (5)
O2—C8 (Å)	1.446 (11)	1.470 (5)
C2—C7═O1 (°)	124.4 (9)	123.1 (5)
C2—C7—O2 (°)	112.3 (10)	110.2 (5)
O1═C7—O2 (°)	123.3 (13)	126.5 (5)
C7—O2—C8 (°)	116.2 (11)	113.0 (5)
|C3—C2—C7—O1| (°)	5.7 (34)	16

Table 9. *Methyl 2-naphthoate conformations in the CSD*

Refcode	Molecule	'C3—C2—C7—O1' torsion angle (°)
ACNPHA	Methyl-4-acetoxy-8-iodo-5,7-dimethoxy-2-naphthoate (Cameron *et al.*, 1981)	2.0
ACNPHB	Methyl-4-hydroxy-8-iodo-5,7-dimethoxy-2-naphthoate (Cameron *et al.*, 1981)	170.5
ACNPHD	Methyl-4-acetoxy-8-iodo-5,6,7-trimethoxy-2-naphthoate (Cameron *et al.*, 1981)	5.6, 9.9
ACNPHE	Methyl-8-iodo-4,5,6,7-tetramethoxy-2-naphthoate (Cameron *et al.*, 1981)	−2.1, 2.2
JOTFUT	Methyl 8-((2,7-dimethoxynaphthyl)ethynyl)-7-methoxy-2-naphthoate (Prince, Fronczek & Gandour, 1992)	173.7
KOTRAM	Methyl 8-((2,6-dimethoxyphenyl)ethynyl)-7-methoxy-2-naphthoate (Prince, Evans *et al.*, 1992)	−6.3
KUXGIT	Methyl 4-(3,4-dimethoxyphenyl)-6,7-dimethoxynaphthalene-2-carboxylate (Sakakibara *et al.*, 1991)	−172.8
TEBFUB	Methyl 7-methoxy-2-naphthoate (Prince *et al.*, 1991)	−1.5
ZAMWOZ	(*R*)-Methyl 6-((4-bromobenzoyloxy)(5,5,8,8-tetramethyl-5,6,7,8-tetrahydro-2-naphthyl)methyl)-2-naphthalenecarboxylate (Gao *et al.*, 1995)	−10.7

of the ring plane) in an analysis of the conformation. The carboxylic acid groups on average are twisted 5.5 (43)° out of the aromatic plane. The apparent C1—C2—C7═O1 torsion angle of 20° is much larger than

Table 10. *Dimethyl 2,6-naphthalenedicarboxylate rotor study optimized energy (kJ mol^{-1})*

Angle (°)	ΔE(AM1)	ΔE(HF)	ΔE(MP2)	AM1	HF 3-21G*	MP2/3-21G*
0	0.00	0.00	0.00	−522.591	−3480.447	−3487.496
10	0.46	2.80	2.26	−522.127	−3480.443	−3487.492
20	1.88	11.08	8.95	−520.705	−3480.426	−3487.479
30	4.31	24.18	19.45	−518.270	−3480.405	−3487.462
40	7.66	41.04	32.96	−514.949	−3480.380	−3487.441
50	11.50	60.28	48.28	−511.087	−3480.351	−3487.416
60	15.35	79.94	63.96	−507.239	−3480.317	−3487.391
70	18.57	97.72	78.27	−504.034	−3480.288	−3487.370
80	20.66	110.73	88.89	−501.942	−3480.267	−3487.354
90	21.38	114.75	92.11	−501.211	−3480.262	−3487.349

this average, but this large value is probably an artifact of NDA disorder.

A similar search of the CSD for aromatic methyl esters containing no *ortho* substituents yielded 68 hits. The average twist angle of the methyl ester out of the aromatic ring plane is 5.7 (34)° (Table 8). Among these aromatic methyl esters are nine methyl 2-naphthoates. Of the 11 independent molecules in these structures, eight have ester conformations similar to that observed in NDC. Since the *Z* conformation of NDC packs better, it may also do so in other structures and thus be predominant in the solid state. The observed value of the C3—C2—C7═O1 torsion angle of 16° is the largest observed so far (Table 9). It is of some interest to quantify the energy cost of this twist.

Conformational analyses of the C3—C2—C7═O1 bond in NDC [carried out using both *SYBYL* (Tripos Associates Inc., 1994; Tripos force field) and *Cerius*^{2} (Molecular Simulations Inc., 1995; Dreiding II force field) indicate that torsion angles of 0 (*Z*) and 180° (*E*) are the local minima and that these conformations have identical energy. The shapes of the curves of conformational energy *versus* torsion angle were identical from the two programs, but the calculated energy differences differed. *SYBYL* (Tripos Associates Inc., 1994) yielded a difference between the 0/180 and 90° conformations of 23.0 kJ mol^{-1}, while *Cerius*^{2} (Molecular Simulations Inc., 1995) yielded a value of 41.5 kJ mol^{-1}.

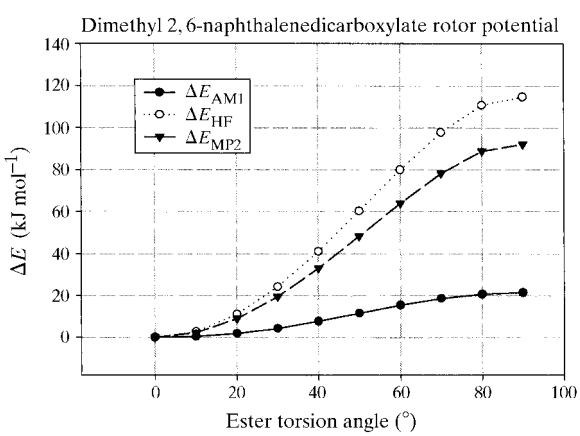

Fig. 10. The conformational energy of NDC from AM1, Hartree–Fock (HF) and MP2 calculations.

Although the literature on torsional energy barriers in aromatic carboxyl compounds is not extensive, both experimental and theoretical studies indicate energy barriers in the range 16–50 kJ mol^{-1} (Drakenberg *et al.*, 1980; Barthelemy *et al.*, 1978). Since electronic effects undoubtedly play an important part in determining the 'stiffness' of the $C_{arom}—C_{carb}$ (where arom = aromatic and carb = carboxyl) bond, molecular mechanics tools are not the best for such energy barrier calculations; quantum mechanical calculations are necessary. Both experimental data and calculations on benzaldehyde suggest that satisfactory agreement between observed and calculated energy barriers at the *ab initio* level requires in general very extensive calculations, including electron correlation at the MCSCF level (Coussens *et al.*, 1992). Such calculations are impractical to use as a regular tool for conformational analysis, so semi-empirical methods have been evaluated for their utility in predicting the conformational energy barriers in carbonyl-substituted aromatic compounds (Coussens *et al.*, 1992; Leiva *et al.*, 1996). Good agreement between the experimental and AM1 calculated rotational barriers can be obtained by multiplying the latter by a factor of 1.9 (Coussens *et al.*, 1992). A good correlation (estimated standard uncertainty = 1.08 kJ mol^{-1}) between experimental ΔG and V_{AM1} potential energy barriers has been obtained for a series of aromatic carbonyl compounds (Leiva *et al.*, 1996) according to

$$\Delta G \text{ (kJ mol}^{-1}) = 2.24\ (8) V_{AM1} + 7.79\ (84).$$

In all cases the minimum energy conformation was the planar geometry and the maximum energy conformation showed a torsion angle of 90°. These two correlations result in differences of 10 kJ mol^{-1} when applied to an individual calculated energy barrier. It has been noted that in the solid state torsional barriers can be as large as twice those obtained in the gas phase (Lautenschläger *et al.*, 1991; Miller *et al.*, 1967).

The conformational energy diagram of NDC was calculated using *SPARTAN*'s (Wavefunction Inc., 1995) coordinate driving methodology. With this technique, geometric variables (*e.g.* dihedral angles) are ratcheted through a sequence of constrained structures, such that

an examination of the variation in molecular energy as a function of these variables is performed. To estimate the torsional energy barrier in NDC, the ester groups were rotated out of the plane of the aromatic rings in 10° increments and each structure fully converged subject to the geometrical constraints. The torsion range 0–90° was covered using AM1 (Dewar *et al.*, 1985) and Hartree–Fock (Hehre *et al.*, 1986; Szabo & Ostlund, 1982; Levine, 1991) (HF/3-21G) methods as implemented in *SPARTAN* (Wavefunction Inc., 1995). To estimate the effect of inclusion of correlation energy on the rotational barrier estimates, single point MP2/3-21G calculations at the optimized HF/3-21G geometries were performed using *GAMESS* (Schmidt *et al.*, 1990, 1993; Table 10 and Fig. 10).

For the observed torsion angle of 20°, AM1 predicts an increase in energy of 1.88 kJ mol^{-1}, HF/3-21G predicts 11.09 kJ mol^{-1} and MP2/3-21G single point predicts 8.95 kJ mol^{-1}. These energy changes refer to whole molecules and include contributions from two rotating ester groups. The MP2/3-21G single-point calculations represent our best estimate of the energy change caused by rotating the ester groups out of the naphthalene plane, approximately 9 kJ mol^{-1}.

Even though the completely planar conformation of the NDC molecule seems to be preferred in the gas phase, rotation of the ester linkage out of the plane requires only a small increase in energy. The observed torsion angle of 20° represents an increase in conformational energy of 9 kJ mol^{-1}, a small penalty to pay for a greatly improved crystal packing.

4. Discussion

The crystal structures of 2,6-dimethylnaphthalene (DMN), 2,6-naphthalenedicarboxylic acid (NDA) and dimethyl 2,6-naphthalenedicarboxylate (NDC) have been determined and refined using a combination of computational and experimental techniques. The structures provide the basis for quantitative analysis methods using powder diffraction techniques and make possible understanding of the nature of the defects and faulting in the materials. In addition, the crystal structures enable the prediction of crystal morphology.

These structure solutions demonstrate that computational tools have advanced enough to be of real assistance in the solution of organic crystal structures using powder diffraction data. The availability of such tools will permit the solution of the structures of compounds which do not form good single crystals. Many important compounds fall into this category.

Statistical and computational studies demonstrate that the aromatic–carboxyl linkage is relatively flexible. In the observed structure of NDC the ester group is twisted 20° out of the mean plane of the naphthalene ring. This twist 'costs' 9 kJ mol^{-1} and permits much better crystal packing. An appreciation of the flexibility of such linkages should prove useful in interpreting polyester properties.

We thank Ying-Mei Chen for technical assistance and collection of the synchrotron pattern of NDC, and T. E. Wolff for literature surveys. P. W. Stephens, Robert Dinnebier and Götz Bendele were most gracious and helpful during the collection of the synchrotron data. J. M. Wies, D. J. Schneider, R. F. McMahon, R. C. Feld and R. B. Edlund provided the samples on which this work was based. D. L. Sikkenga synthesized the NDA from which the lattice parameters were determined and provided encouragement for this work. This work represents research carried out in part at the National Synchrotron Light Source at Brookhaven National Laboratory, which is supported by the US Department of Energy, Division of Materials Sciences, and Division of Chemical Sciences. The SUNY X3 PRT beamline at NSLS is supported by the Division of Basic Energy Sciences of the US Department of Energy (grant DE-FG02-86ER-45231).

References

Allen, F. H. & Kennard, O. (1993). *Chem. Des. Autom. News*, **8**, 31–37.

Barthelemy, J.-F., Jost, R. & Sommer, J. (1978). *J. Org. Magn. Reson.* **11**, 438–442.

Boultif, A. & Louer, D. (1991). *J. Appl. Cryst.* **24**, 987–993.

Cameron, D. W., Feutrill, G. I., Pannan, L. J. H., Raston, C. L., Skelton, B. W. & White, A. H. (1981). *J. Chem. Soc. Perkin Trans.* 2, pp. 610–627.

Coussens, B., Pierloot, K. & Meier, R. J. (1992). *J. Mol. Struct. (Theochem.)*, **259**, 331–344.

Dewar, M. J. S., Zoebisch, E. G., Healy, E. F. & Stewart, J. J. P. (1985). *J. Am. Chem. Soc.* **107**, 3902–3909.

Drakenberg, T., Sommer, J. & Jost, R. (1980). *J. Chem. Soc. Perkin Trans.* 2, pp. 363–369.

Gao, Q., Yu, K.-L., Mansuri, M. M., Kerns, E. H. & Starrett, J. E. (1995). *Acta Cryst.* C**51**, 1672–1675.

Hehre, W., Radom, L., Schleyer, P. & Pople, J. (1986). *Ab Initio Molecular Quantum Theory*. New York: Wiley and Sons.

Kitaigorodskii, A. I. (1946). *Isv. Akad. SSSR Otd. Khim. Nauk*, p. 587.

Kitaigorodskii, A. I. (1953). *Struct. Rep.* **10**, 280.

Larson, A. C. & Von Dreele, R. B. (1994). *GSAS. The General Structure Analysis System*. Los Alamos National Laboratory, Los Alamos, USA.

Lautenschläger, P., Brickman, J., van Ruiten, J. & Meier, R. J. (1991). *Macromolecules*, **24**, 1284–1292.

Leiva, M. A., Morales, R. G. E. & Vargas, V. (1996). *J. Phys. Org. Chem.* **9**, 455–458.

Levine, I. (1991). *Quantum Chemistry*, 4th ed. Englewood Cliffs, New Jersey: Prentice-Hall.

Miller, F. A., Fateley, W. G. & Witkowski, R. E. (1967). *Spectrochim. Acta Part A*, **23**, 891–908.

Molecular Simulations Inc. (1995). *Cerius*^{2}. Version 2.0. Molecular Simulations Inc., 9685 Scranton Road, San Diego, CA 92121, USA.

Morse, P. M. (1997). *Chem. Eng. News*, **75**, 8–9.
Prince, P., Evans, K. L., Fronczek, F. R. & Gandour, R. D. (1992). *Acta Cryst.* C**48**, 936–938.
Prince, P., Fronczek, F. R. & Gandour, R. D. (1991). *Acta Cryst.* C**47**, 2226–2227.
Prince, P., Fronczek, F. R. & Gandour, R. D. (1992). *Acta Cryst.* C**48**, 1538–1540.
Sakakibara, I., Katsuhara, T., Ikeya, Y., Hayashi, K. & Mitsuhashi, H. (1991). *Phytochemistry*, **30**, 3013–3016.
Schmidt, M., Baldridge, K., Boatz, J., Elbert, S., Gordon, M., Jensen, J., Koseki, S., Matsunaga, N., Nguyen, K., Su, S., Windus, T., Dupuis, M. & Montgomery, J. (1993). *J. Comput. Chem.* **14**, 1347–1363.
Schmidt, M., Baldridge, K., Boatz, J., Jensen, J., Koseki, S., Gordon, M., Nguyen, K., Windus, T. & Elbert, S. (1990). *QCPE Bull.* **10**, 52.
Sheldrick, G. M. (1988). *SHELXTL-Plus*88 *Structure Determination Software Programs*. Nicolet Instrument Corporation, Madison, Wisconsin, USA.
Szabo, A. & Ostlund, N. (1982). *Modern Quantum Chemistry*. New York: MacMillan.
Tripos Associates Inc. (1994). *SYBYL*. Version 6.1. Tripos Associates Inc., 1699 S. Hanley Road, St Louis, MO 63144, USA.
Visser, J. W. (1969). *J. Appl. Cryst.* **2**, 89–95.
Wavefunction Inc. (1995). *SPARTAN*. Version 4.1. Wavefunction Inc., 18401 Von Karman Avenue, Suite 370, Irvine, CA 92612, USA.